

Beta Decay of F^{20} †

CALVIN WONG*

Kellogg Radiation Laboratory, California Institute of Technology, Pasadena, California

(Received February 1, 1954; revised manuscript received April 13, 1954)

The beta decay of F^{20} has been investigated with a magnetic lens spectrometer. The decay proceeds mainly to the first excited state of Ne^{20} by a beta ray of maximum energy 5.419 ± 0.013 Mev, followed by a gamma ray of energy 1.627 ± 0.005 Mev. The excited state transition, with comparative half-life $ft = 9.73 \times 10^4$ seconds, has the allowed shape down to 1 Mev.

A magnetically compensated stilbene scintillation counter has been employed to show that the counts beyond the end point of the intense beta component are due predominantly to scattered electrons and room background. The direct transition to the ground state of Ne^{20} ($Q = 7.047 \pm 0.014$ Mev) is estimated to have a relative intensity of less than $\sim 3.2 \times 10^{-4}$ of the excited state transition, corresponding to a comparative half-life $ft \gtrsim 10^9$ seconds.

INTRODUCTION

THE beta decay of F^{20} has been investigated most recently by Alburger¹ who reports that the decay proceeds mainly to the first excited state of Ne^{20} by a beta ray of 5.406 ± 0.017 -Mev maximum energy, followed by a gamma ray of energy 1.631 ± 0.006 Mev. The Fermi plot is linear above about 2.5 Mev and direct transitions to the ground state comprise less than 1 percent, according to this work. In the present paper is reported a parallel investigation which confirms Alburger's results concerning the nature of the decay, enables a somewhat lower limit to be placed on the fraction of direct transitions to the ground state, and establishes the linearity of the Fermi plot to lower energies.

EXPERIMENTAL METHOD

Radioactive F^{20} ($\tau_{1/2} = 11.4$ sec) was produced by the $F^{19}(d,p)F^{20}$ reaction; CaF_2 targets were bombarded with 2.3-Mev deuterons from the 3-Mev Kellogg Radiation Laboratory electrostatic generator. The deuteron beam was brought directly into the vacuum chamber of the spectrometer to bombard targets at the source position. The beta-ray spectrometer, which is described in an earlier paper,² had a resolution of 2 percent, and the effective solid angle was 2.5 percent of a sphere. Helical baffles permit observation of electrons and positrons separately. The momentum calibration was obtained from the average of three independent determinations of the peak position of the internal conversion "X" line of Th-D, $B\rho = 9988.4 \pm 2$ gauss-cm. The compensation for the vertical component of the earth's magnetic field was checked by running the Th-C "I" and "F" lines (222 and 147 kev, respectively), and was found to be satisfactory as evidenced by the fact that the resolution for these lines was the same as that for the high-energy "X" line.

The electron detector was a magnetically compensated stilbene scintillation counter. The stilbene crystal was cylindrical in shape having a diameter and height of one inch. A 57-cm Lucite light pipe was employed to allow operation of the 5819 phototube in a region of comparatively weak magnetic field. The spectrometer field in the region of the phototube was then compensated by employing a suitably designed solenoid connected electrically in parallel with the spectrometer coils. The compensation was checked by placing a gamma-ray source in a fixed position external to the spectrometer proper and observing the counting rate as a function of spectrometer current. Even for the highest currents utilized in the present experiment, the counting rates were constant, showing that the counter sensitivity was not a function of spectrometer current. It was found that the pulse-height output of the counter was directly proportional to the energy of the electrons being focused in the range $E_\beta = 0.2$ to 6 Mev. This useful property enables one to distinguish between direct and scattered electrons, since the latter are usually much degraded in energy. One has only to run integral bias curves and see whether or not the integral bias steps move properly with respect to the energy of the electrons supposedly being focused. The monitor counter was a conventional Geiger counter which was shielded by lead, except in the direction of the target, to reduce its background counting rate.

Primarily to avoid counting the intense prompt radiation, the counters were turned off during the 6-second bombardment period. An 0.2-second delay was introduced between the end of the bombardment and the turning on of the counters to insure that only the delayed radiation was being counted and monitored. During the 5.8-second counting period, the deuteron beam was intercepted by a tantalum-backed beam chopper. This cycle was repeated until the monitor counter recorded a fixed number of gamma-ray counts, which indicated that a certain number of beta disintegrations had occurred. The turning on and off of the counters and the operation of the beam chopper

† Assisted by the joint program of the U. S. Office of Naval Research and the U. S. Atomic Energy Commission.

* Present address: University of California Radiation Laboratory, Livermore, California.

¹ D. E. Alburger, Phys. Rev. **88**, 1257 (1952).

² Hornyak, Lauritsen, and Rasmussen, Phys. Rev. **76**, 731 (1949).

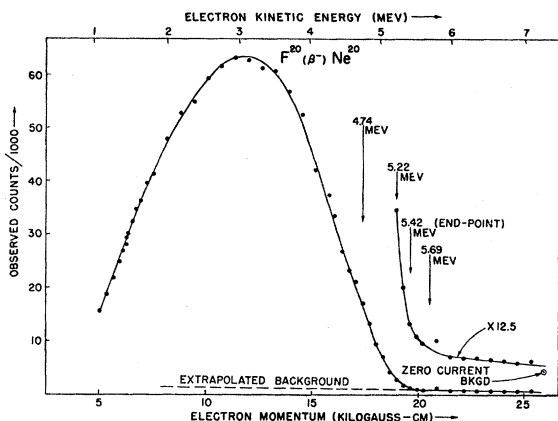


FIG. 1. Electron spectrum from the beta decay of F^{20} . The spectrum was run with a counter bias of 10 volts which corresponds to counting all electrons with energies ≥ 900 kev. The zero current background has not been subtracted from the spectrum.

were accomplished by a system of relays actuated by a synchronous motor.

ELECTRON SPECTRUM

For the beta-spectrum measurements, a thin layer of CaF_2 was evaporated on 0.1-mil nickel foil. This foil was then supported by a 5-mil aluminum foil which had a $\frac{3}{8}$ -inch hole in its center. The observed spectrum, displayed in Fig. 1, shows the main component having an end point at about 5.42 Mev and a tail extending to higher energies. The tail eventually runs into the zero current background which represents the sum of room background plus gamma-ray background from the $F^{20}(\beta^-)Ne^{20*}$ reaction. The field-sensitive part of the tail, particularly the broad fillet in the region of 5.69 Mev, is attributed either to scattered electrons or to the ground-state transition ($Q=7.05$ Mev). In order to determine to what extent scattering is present, the energy distribution of the electrons at a spectrometer setting of 5.69 Mev was analyzed by running an integral bias curve with the scintillation counter detector. For

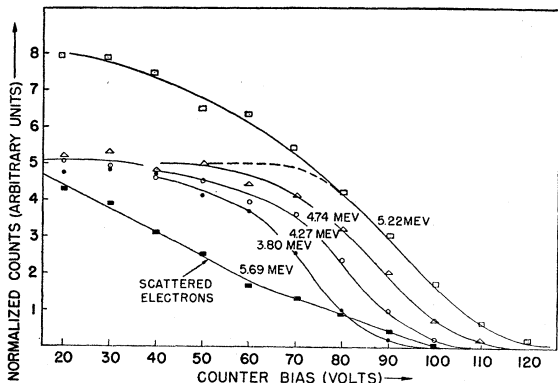


FIG. 2. Integral bias curves of the F^{20} beta spectrum. The dashed portion of the 5.22-Mev curve represents what would be observed if scattered electrons were not present.

purposes of comparison, integral bias curves were also run at spectrometer settings corresponding to 5.22, 4.74, 4.27, and 3.80 Mev. The results are shown in Fig. 2, where the curves have been normalized in accordance with the beta spectrum of Fig. 1. In addition, the curves have been corrected for room background and gamma-ray background from the $F^{20}(\beta^-)Ne^{20*}$ reaction by subtracting the zero current integral bias curve from the observed bias curves. As can be inferred from Fig. 1, the zero current background correction was negligible in the case of the three lower energy curves of Fig. 2 because of the relatively large number of beta counts.

At 4.74 Mev, for example, where it is clear from Fig. 1 that most of the counts are due to focused electrons, the bias curve displays a reasonably flat plateau indicating that the electrons are monoenergetic. The half-value point, 87 volts, agrees with that expected from the energy calibration of the crystal and the

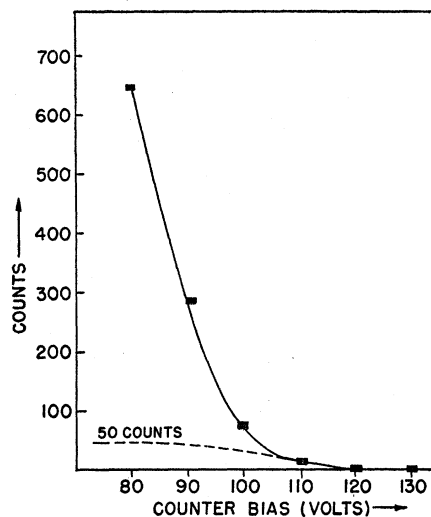


FIG. 3. The 5.69-Mev bias curve plotted on an expanded vertical scale in the region beyond 80 volts.

momentum setting of the spectrometer. At 5.69 Mev, however, it is apparent that focused electrons are almost totally absent since the bias curve does not display the integral bias step expected from 5.69-Mev electrons. Furthermore, since the integral bias curve is a sloping straight line, its differential bias curve is a rectangle which indicates that, below approximately 4 Mev, electrons of all energies are present in equal amounts. This again suggests that the counts recorded at 5.69 Mev, after subtracting the zero current background, are due predominantly to scattered electrons. The 5.22-Mev curve, on the other hand, shows a transition shape consistent with the expectation from extrapolating the fillet of Fig. 1 that about a third of the recorded counts, after subtracting the zero current background, are due to scattered electrons. In order to establish a rough upper limit on the number of true 5.69-Mev electrons that could be present, one may fit a calculated 5.69-Mev

bias step to the observed bias curve at a point where the bias step should reach half-maximum, i.e., at approximately 105 volts. This is depicted in Fig. 3, where the 50 counts represent the maximum admixture of 5.69-Mev electrons allowable on the basis of the observed integral bias curve. Comparing this figure with the 374 000 counts observed at the peak of the excited state component, and assuming an allowed shape for the ground-state transition, a rough upper bound of 3.2×10^{-4} is obtained for the ground-state branching ratio. On the basis of the present experimental evidence, it cannot be said that the branching ratio is equal to 3.2×10^{-4} since the 5.69-Mev curve does not show enough structure to make possible a positive identification.

Since scattering was shown to be present, its effect upon spectrum shape and measured end point was determined experimentally by running the beta spectra of Na²² and P³². The Na²² Fermi plot, Fig. 4, is linear down to 200 kev, and the 540-kev end point is in agreement with the currently accepted value of 542 ± 5 kev.³ The P³² Fermi plot, not displayed, is linear down to 330 kev, and the 1.714 ± 0.006 Mev end point is in

TABLE I. Contributions of various sources of error.

Source of error	Error in end point (Mev)
Background	± 0.010
Calibration	± 0.006
Error in fitting Kurie plot (above 2.8 Mev)	± 0.005
Statistical	± 0.004
Total probable error in end point	± 0.013

agreement with the 1.707 ± 0.004 -Mev value quoted by Li.⁴ The effects of scattering upon spectrum shape and measured end point are thus negligible above about 300 kev.

The background correction for the beta spectrum was obtained by a straight line extrapolation of the high-energy tail to lower energies as shown in Fig. 1. This method of background subtraction has no *a priori* justification except that its application to the Na²² and P³² beta spectra gave end points in good agreement with currently accepted values. From Fig. 1, it is evident that the zero current background accounts for the major part of the extrapolated background. Subtracting the high-energy tail and the extrapolated background and making the usual Fermi plot yielded the straight line of Fig. 5. A straight line fits the data from the end point down to 1 Mev. The values of the Fermi function $f = F\beta^2$ were obtained from tables published by the National Bureau of Standards.⁵ A least-squares analysis

³ Macklin, Lidofsky, and Wu, Phys. Rev. 78, 318 (1950).

⁴ C. W. Li, Phys. Rev. 88, 1038 (1952).

⁵ Tables for the Analysis of Beta Spectra, National Bureau of Standards; Applied Mathematics Series (U. S. Government Printing Office, Washington, D. C., 1952), Vol. 13.

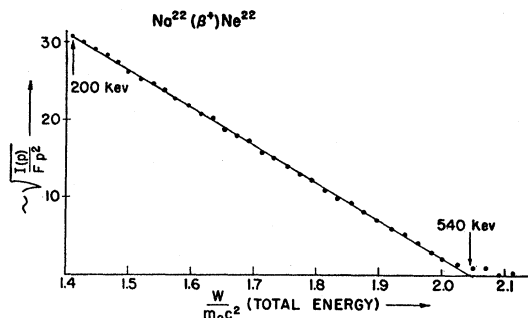


FIG. 4. Fermi-Kurie plot of the Na²² positron spectrum.

of four sets of data between 2.8 and 5.4 Mev gave an end-point energy of 5.419 ± 0.013 Mev. The end-point value includes a three kev correction for energy loss in the Ni foil. The data below 2.8 Mev usually displayed more scattering and hence were disregarded in the least-squares solutions for the end point. Table I shows how the various sources of error contribute to the final probable error of ± 0.013 Mev.

The principal source of uncertainty in the end-point value lies in the estimate of background: a variation of a factor of two in the background value assumed would not have noticeably affected the straightness of the plot, but would have changed the apparent end point by 14 kev. Due to difficulty in estimating the exact contribution from scattered electrons throughout the spectrum, the background in the present case is uncertain to about ± 70 percent, and the resulting uncertainty in the end point is ± 10 kev. It may be remarked this source of error seems to have been frequently disregarded in the literature and may account for some of the discrepancies which have appeared in β -ray end point determinations.

GAMMA-RADIATION SPECTRUM

For the delayed gamma-ray measurements, a 40-mil CaF₂ crystal, 150-mil copper absorber, and a 23.2-mg/cm² thorium converter were used. The observed

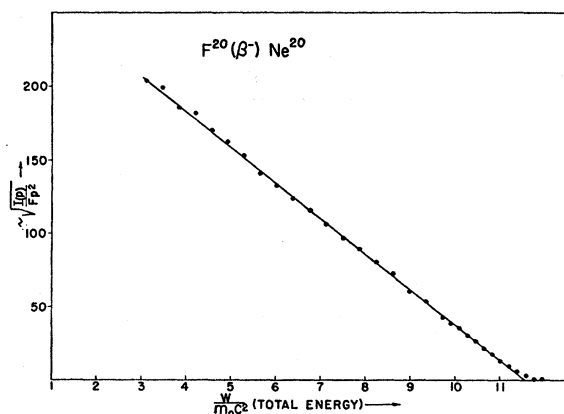


FIG. 5. A typical Fermi-Kurie plot of the F²⁰ electron spectrum.

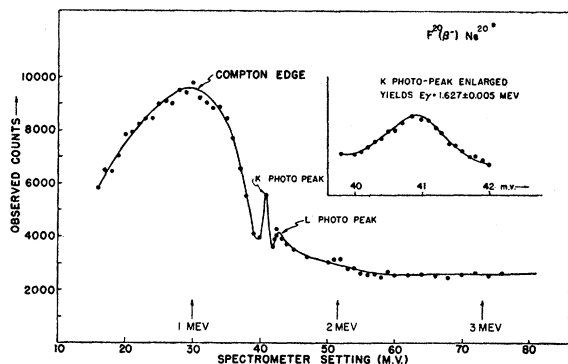


FIG. 6. Gamma radiation from the beta decay of F^{20} . In the upper right-hand corner, the K photopeak is shown enlarged.

spectrum, shown in Fig. 6, shows the Compton edge, K and L photopeaks from a single gamma ray. The gamma-ray energy was obtained by adding the K binding energy of thorium plus a converter shift correction² to the measured energy of the K photoelectrons. An average of four independent determinations yielded 1.627 ± 0.005 Mev as the gamma-ray energy. The position of the Compton edge is consistent with a gamma ray of this energy.

As a check on the accuracy of the gamma-ray measurements, the Co^{60} K photoelectric peak was run using the same absorber and converter geometry. An average of two determinations gave 1.332 Mev as the gamma-ray energy, in good agreement with the currently accepted value of 1.3325 ± 0.0003 Mev.⁶

DISCUSSION

The present investigation confirms that the decay proceeds mainly to the first excited state of Ne^{20} by a beta ray of maximum energy 5.419 ± 0.013 Mev, followed by a gamma ray of energy 1.627 ± 0.005 Mev. The Fermi plot is linear down to 1 Mev, and direct transitions to the ground state is estimated to have a relative intensity of less than 3.2×10^{-4} of the excited state transition.

Comparison with the results of Alburger shows substantial agreement, both qualitatively as regards the decay scheme and quantitatively as regards the beta-ray end point and gamma-ray energy. Although consistent with Alburger's estimate of less than 1 percent, the

⁶ Lindström, Hedgran, and Alburger, Phys. Rev. **89**, 1303 (1953).

upper limit for the ground-state branching ratio is now a factor of thirty smaller. As regards the Fermi plot, it is not obvious why Alburger's plot deviates from linearity at approximately 2.5 Mev; the target thicknesses were comparable while the source backing was twice as thick in the present experiment.

Adding a 1-kev correction for the Ne^{20} recoil (the calculated correction being 0.92 kev), the $F^{20}-Ne^{20}$ atomic mass difference is 7.047 ± 0.014 Mev. Using, in addition, the Q values for the $F^{19}(d,p)F^{20}$ and $Ne^{20}(d,p)Ne^{21}$ reactions,⁴ the predicted Q value for the $Ne^{21}(d,\alpha)F^{19}$ reaction is 6.442 ± 0.019 Mev. This is in agreement with the value determined by Whaling and Mileikowsky: 6.432 ± 0.010 Mev.⁷

Since Alburger's publication, two additional pieces of information affecting the F^{20} beta decay have become available. Seed⁸ and Richards⁹ report that the Ne^{20} first excited state has the assignment $2+$. Bromley *et al.*,¹⁰ applying the Butler stripping theory to the $F^{19}(d,p)F^{20}$ reaction, report that the F^{20} ground state has the assignment $1+$. The excited state transition is thus $\Delta J=1$; no parity change, and hence allowed. This agrees with the experimental evidence: the Fermi plot is linear down to 1 Mev and the comparative half-life ft equals 9.73×10^4 seconds ($E_{\beta \text{ max}} = 5.42$ Mev and $\tau_{1/2} = 11.4$ seconds). Since the Ne^{20} ground state is $0+$, the ground-state transition is also $\Delta J=1$; no parity change, and hence should be allowed. However, the upper limit of 3.2×10^{-4} for the ground-state branching ratio yields a comparative half-life $ft \gtrsim 10^9$ seconds. The ground-state transition appears then to be at least first forbidden. A possible explanation for the apparent anomaly is that the transition is l forbidden. Nordheim¹¹ lists 7 ground-state transitions involving even- A nuclei as l forbidden with $\log ft$ ranging from 5.0 to 9.0.

The author is grateful to W. Whaling for suggesting the problem and to T. Lauritsen for guidance during the course of the experiment. He is also grateful to C. Mileikowsky, W. A. Fowler, and R. F. Christy for helpful discussion. In particular, he is indebted to D. E. Alburger for communicating his results prior to publication, and for his helpful criticism about experimental technique.

⁷ C. Mileikowsky and W. Whaling, Phys. Rev. **88**, 1254 (1952).

⁸ J. Seed, Phil. Mag. **44**, 921 (1953).

⁹ H. T. Richards, Indiana University Conference, 1953 (unpublished).

¹⁰ Bromley, Bruner, and Fulbright, Phys. Rev. **89**, 396 (1953).

¹¹ L. W. Nordheim, Revs. Modern Phys. **23**, 322 (1951).